Transition probabilities of the $3p$-$3s$ transitions of Ne I*†

S. Inatsugu and J. R. Holmes
Department of Physics and Astronomy, University of Hawaii, Honolulu, Hawaii 96822
(Received 23 October 1973; revised manuscript received 12 August 1974)

Transition probabilities for the $3p$-$3s$ array of Ne I have been measured in emission from a glow discharge containing a He-Ne-Ar mixture. The neon spontaneous emission at 632.8 nm ($3s_2$-$2p_4$) was taken as the reference line and the emission intensities of the $2p_i$-$1s_j$ lines were compared with it to obtain the relative transition probabilities $A(2p_i\text{-}1s_j)/A_{632.8}$. The discharge condition was carefully controlled so that the ratio of the populations of the $3s_2$ and a given $2p_i$ level was precisely equal to the ratio of the statistical weights of the energy levels: $N(3s_2)/N(2p_i) = g(3s_2)/g(2p_i)$, eliminating two population unknowns encountered in an ordinary gas discharge. The relative A values were then converted to the absolute values by means of the accurate value of $A_{632.8}$, which was obtained in our recent measurements. The results were subjected to extensive comparisons with other experimental data of Bridges and Wiese, of Bennett and Kindlmann, and the intermediate coupling calculations by Mehlhorn and by Feneuille *et al*. Excellent agreement was observed throughout between these data sets and our results. The following has been found: Our results are more consistent with the J-file–sum rule than any other experimental data; our relative line strengths are in excellent agreement with the theoretical calculations of Feneuille *et al*.; our radial transition integral σ^2 exhibits least variations over different $2p$ levels—its weighted average has been found to be 6.66 ± 0.02 (a.u.) on an absolute basis, which is very close to the value obtained from the Coulomb approximation; and our transition-probability sums are in excellent agreement with those evaluated from the intermediate coupling calculations combined with the Coulomb approximation. Based on these findings and the error analysis, we estimate the uncertainty of our A values, except for a few weak lines, to be 2% on the relative scale and 6% on the absolute scale. Also, a discussion is given concerning the extent of configuration interaction on the $2p^53p$ states.

I. INTRODUCTION

Many attempts have been made, both in theory and in experiments, to acquire a better understanding of the angular-momentum coupling scheme in Ne I. Experimental results have indicated that none of the pure coupling schemes proposed thus far, such as jl or jK coupling, could provide an accurate description for the configurations of $2p^5np$ electrons in neon and the p^5p-type configurations in heavier rare gases.

The intermediate coupling scheme of Shortley[1] proved to be a more realistic description of the rare-gas spectra. Especially during recent years, the extensive use of electronic computers has improved theoretical results[2-4] based on the intermediate coupling scheme. On the other hand, despite numerous experimental attempts[5] using various techniques, a wide margin of error has persisted in the radiative transition probabilities and lifetimes for the $3p$-$3s$ array of Ne I, oftentimes frustrating further theoretical endeavors.

The conventional methods such as emission and absorption techniques must unavoidably encounter the formidable task of absolute measurements of intensities, particle densities, temperature, etc., in order to link the transitions arising from various upper levels. Such a procedure is subject to various systematic errors. Among many works conducted in recent years, the best experimental data may be the lifetimes obtained by Bennett and Kindlmann,[6] who have reduced the error to a few percent, and also the relative transition probabilities obtained by Bridges and Wiese,[7] who have established, through a common temperature value, the relative scale of A values for the lines originating from the ten energy levels of $3p$ electrons. The uncertainty estimated for these relative values was 7%. However, a further reduction of the error is necessary in order to examine, for instance, the effect of configuration interaction that has been suspected to be present at a significant level among the $2p^5np$ configurations in neon.

We present in this paper a set of accurate transition probabilities for the $3p$-$3s$ array of Ne I, obtained by means of a new experimental method which is intrinsically free from those systematic errors. The method employs a laser radiation as a probe to determine exactly the relative population densities of a pair of excited states in a gas discharge, thereby enabling one to measure the relative transition probabilities of lines arising from two different upper levels. The technique was originally used by Hänsch and Toschek[8] and Bychkova *et al*.[9] in their attempt to measure the transition probability of the popular He-Ne laser line at 632.8 nm ($3s_2$-$2p_4$) in relation with the known transition probability of the $2p_4$-$1s_4$ line. Recently we have improved this technique and demonstrated its potential capability.[10]

II. EXPERIMENTAL METHOD

In this section, a rate-equation analysis similar to that given in Ref. 10 is treated for a general case.

Consider a pair of energy levels, denoted by $|1\rangle$ and $|2\rangle$, between which a laser oscillation is possible. Assume that level $|1\rangle$ lies higher than level $|2\rangle$. In a glow-discharge regime, the populations of these levels attain steady state through detailed balancing between excitation and deexcitation mechanisms.

Suppose there are N_1' atoms/cm^3 in level $|1\rangle$ and N_2' atoms/cm^3 in level $|2\rangle$ at steady state. These atoms are constantly created at the rates R_1 and R_2 (atoms/cm^3 sec), respectively, via electron impact upon ground-state atoms, radiative cascading from higher levels, and any other possible means. At the same time, they undergo destruction via collisional and radiative decay processes at the rates W_1N_1' atoms/cm^3 sec and W_2N_2' atoms/cm^3 sec, where W_1 and W_2 are the total deexcitation coefficients of level $|1\rangle$ and level $|2\rangle$, respectively. Thus, at steady state, the following relationships exist:

$$0=\dot{N}_1'=R_1-W_1N_1', \tag{1}$$

$$0=\dot{N}_2'=R_2-W_2N_2'+C_{12}N_1', \tag{2}$$

where $C_{12}N_1'$ is the rate of excitation of level $|2\rangle$ by a direct and indirect radiative cascading from level $|1\rangle$. This cascade term, which could be included in R_2, is shown explicitly because it involves N_1' directly. There are also other terms in R_1 and R_2 that may involve N_1' and N_2' directly (collisions of the second kind between levels $|1\rangle$ and $|2\rangle$, for example), but these terms are usually negligibly small. The coefficient C_{12} may be approximated by A_{12}, the spontaneous transition probability of Einstein, if the process is dominated by the direct cascading.

If a strong quasimonochromatic radiation field, such as from a laser, having energy density $\rho(\nu)$ centered at frequency ν_{12} is introduced into such a steady-state plasma, the radiation field, being in resonance with levels $|1\rangle$ and $|2\rangle$, will be either absorbed or intensified by stimulated emission, depending on the relative population distribution between the levels. An optical perturbation of this type is highly selective, thus disturbing only the populations of these two levels, while the rest of the energy levels remain unaffected in the first-order approximation. Hence, with the optical field turned on, levels $|1\rangle$ and $|2\rangle$ will attain a new steady-state population, N_1 and N_2, respectively, of which $dN_1(\nu)$ atoms are capable of undergoing stimulated emission in the frequency range ν to $\nu+d\nu$, and $dN_2(\nu)$ atoms are capable of absorbing in the same range. According to Einstein's formulation of emission and absorption, the net perturbation of the level $|1\rangle$ population in this frequency interval may be given by $\rho(\nu)[B_{21}dN_2(\nu)-B_{12}dN_1(\nu)]$, where B_{12} and B_{21} are Einstein coefficients of stimulated emission and absorption, respectively.

Detailed balancing must also exist at steady state for the population elements $dN_1(\nu)$ and $dN_2(\nu)$. Therefore, the differential forms of Eqs. (1) and (2) must hold:

$$0=d\dot{N}_1'(\nu)=dR_1(\nu)-W_1dN_1'(\nu), \tag{3}$$

$$0=d\dot{N}_2'(\nu)=dR_2(\nu)-W_2dN_2'(\nu)+C_{12}dN_1'(\nu), \tag{4}$$

where $dR_1(\nu)$ and $dR_2(\nu)$ are the excitation rates of population elements $dN_1'(\nu)$ and $dN_2'(\nu)$, respectively. And when the optical perturbation is turned on, the steady-state equations (3) and (4) will be modified to accommodate the perturbation term given above:

$$0=d\dot{N}_1(\nu)=dR_1(\nu)-W_1dN_1(\nu)+\rho(\nu)[B_{21}dN_2(\nu)-B_{12}dN_1(\nu)], \tag{5}$$

$$0=d\dot{N}_2(\nu)=dR_2(\nu)-W_2dN_2(\nu)+C_{12}dN_1(\nu)-\rho(\nu)[B_{21}dN_2(\nu)-B_{12}dN_1(\nu)]. \tag{6}$$

Notice that the excitation rates $dR_1(\nu)$ and $dR_2(\nu)$ are not altered by the optical perturbation, since the discharge condition is not altered. This assumption is justified since the correction terms attributable to collisions (which we have neglected) are negligibly small, and eventually they will vanish in any case when the plasma becomes transparent. Taking the difference between Eqs. (3) and (5), and also (4) and (6), yields

$$W_1\Delta[dN_1(\nu)]=\rho(\nu)[B_{21}dN_2(\nu)-B_{12}dN_1(\nu)], \tag{7}$$

$$W_2\Delta[dN_2(\nu)]=C_{12}\Delta[dN_1(\nu)]-\rho(\nu)[B_{21}dN_2(\nu)-B_{12}dN_1(\nu)], \tag{8}$$

where $\Delta[dN_{1,2}(\nu)]=dN_{1,2}(\nu)-dN_{1,2}'(\nu)$.

The differential components $W_1\Delta[dN_1(\nu)]$ and $W_2\Delta[dN_2(\nu)]$ may be recognized as the rates at which the radiation field in the frequency interval $d\nu$ interacts with levels $|1\rangle$ and $|2\rangle$, respectively, under a given plasma condition. In particular, $W_1\Delta[dN_1(\nu)]$ is exactly the net number of field quanta absorbed (emitted), if $W_1\Delta[dN_1(\nu)]>0$ (<0), by the unit volume of the plasma every second. Thus, the radiation density within the slab of plasma having a unit cross-sectional area and a thickness

Δx would undergo a change $\Delta\rho(\nu)d\nu$:

$$\Delta\rho(\nu)d\nu = -W_1\Delta[dN_1(\nu)](h\nu/c)\Delta x, \tag{9}$$

and the fractional change, $-\Delta\rho(\nu)d\nu/\rho(\nu)\Delta x$, may now be identified as the so-called absorption coefficient $k(\nu)d\nu$ in the frequency range ν to $\nu+d\nu$. From Eqs. (7) and (9), one obtains,

$$k(\nu)d\nu = -\Delta\rho(\nu)d\nu/\rho(\nu)\Delta x = (h\nu/c)[B_{21}dN_2(\nu) - B_{12}dN_1(\nu)]. \tag{10}$$

If the statistical weights of levels $|1\rangle$ and $|2\rangle$ are g_1 and g_2, respectively, B_{12} and B_{21} are related by

$$g_1 B_{12} = g_2 B_{21}. \tag{11}$$

Also, B_{12} is related to the spontaneous transition probability A_{12} by

$$A_{12} = (8\pi h\nu_{12}^3/c^3)B_{12}. \tag{12}$$

Equation (10) may be integrated over ν to yield the well-known Füchtbauer-Ladenberg formula:

$$\int_0^\infty k(\nu)\,d\nu = \frac{g_1}{g_2}\,\frac{\lambda_{12}^2}{8\pi}A_{12}N_2\left(1-\frac{g_2N_1}{g_1N_2}\right), \tag{13}$$

where it is assumed that the linewidth $\Delta\nu$ satisfies the condition $\Delta\nu \ll \nu \simeq \nu_{12} = c/\lambda_{12}$.

On the other hand, Eqs. (7) and (8) can be integrated over ν if the line shapes $dN_1(\nu)$ and $dN_2(\nu)$ are known. In a low-pressure glow-discharge condition, line broadening is primarily caused by the Doppler broadening, the pressure broadening, and the natural broadening, the latter two effects being considerably smaller than the Doppler effect. Then, it is reasonable to assume that the distribution of atoms on levels $|1\rangle$ and $|2\rangle$ is given by a simple bell-shaped density function $g(\nu)$, common to both levels, centered about ν_{12} with the width $\Delta\nu$ determined by gas temperature and pressure. If $g(\nu)$ is normalized, $\int g(\nu)\,d\nu = 1$, then the population elements $dN_1(\nu)$ and $dN_2(\nu)$ may be given by $N_1\,g(\nu)d\nu$ and $N_2\,g(\nu)d\nu$, respectively. With appropriate substitutions and integrations over ν, Eqs. (7) and (8) become

$$W_1\Delta N_1 = \kappa(\lambda_{12})\frac{g_1}{g_2}\,\frac{\lambda_{12}^3}{8\pi h}A_{12}N_2\left(1-\frac{g_2N_1}{g_1N_2}\right), \tag{14}$$

$$W_2\Delta N_2 = -\kappa(\lambda_{12})\frac{g_1}{g_2}\,\frac{\lambda_{12}^3}{8\pi h}A_{12}N_2\left(1-\frac{g_2N_1}{g_1N_2}\right)+C_{12}\Delta N_1, \tag{15}$$

where the constant $\kappa(\lambda_{12}) = \int\rho(\nu)g(\nu)\,d\nu$ may be regarded as an effective radiation density of the laser.

Since a laser oscillation is possible between levels $|1\rangle$ and $|2\rangle$, the relative population N_1/N_2 may be varied over a wide latitude in either direction from the laser threshold by adjusting the discharge condition. In order to allow adjustments of discharge parameters without altering the laser oscillation, a small discharge tube, containing a suitable gas mixture and powered independently, may be placed inside the main laser cavity. The discharge parameters to be adjusted are usually the total pressure of the gas, the partial pressures of the component gases, and the discharge current. Selection of these parameters are at the experimenter's disposal.

Suppose the discharge condition is so chosen that the condition

$$N_1/N_2 = g_1/g_2 \tag{16}$$

is created in the plasma; the right-hand sides of Eqs. (13)–(15) vanish exactly. Then, there will be neither absorption nor amplification of the radiation field by the plasma: Such a plasma may be termed "transparent" to the radiation $\kappa(\lambda_{12})$. Consequently, from Eqs. (14) and (15), it is necessary that $\Delta N_1 = \Delta N_2 = 0$ if the plasma is made transparent. The optical perturbation vanishes completely despite the presence of an intense resonance field.

Experimentally, the transparency condition, Eq. (16), may be effectively detected by monitoring one of the spontaneous side-light emissions, I_{1i} or I_{2j}, that originate from levels $|1\rangle$ and $|2\rangle$, and terminate on arbitrary levels $|i\rangle$ and $|j\rangle$, respectively. The "side light" is defined as the intensity component of spectra emitted from the discharge tube in the general direction perpendicular to the axis of the laser cavity. The side-light component I_{1i} or I_{2j} is a direct measure of the population of level $|1\rangle$ or $|2\rangle$, respectively, since

$$I_{1i} = A_{1i}N_1h\nu_{1i}/4\pi, \tag{17}$$

and

$$I_{2j} = A_{2j}N_2h\nu_{2j}/4\pi. \tag{18}$$

By turning "on" and "off" the laser field, the intensities will exhibit changes ΔI_{1i} and ΔI_{2j}, which are directly proportional to the population differentials ΔN_1 and ΔN_2, respectively. Hence, $\Delta I_{1i} = \Delta I_{2j} = 0$ verifies that $\Delta N_1 = \Delta N_2 = 0$.

The intensity ratio I_{1i}/I_{2j} measured at this juncture will determine the relative transition probability of these two emission lines via the following equation:

$$\frac{I_{1i}}{I_{2j}} = \frac{A_{1i}}{A_{2j}}\,\frac{N_1}{N_2}\,\frac{h\nu_{1i}}{h\nu_{2j}} = \frac{A_{1i}}{A_{2j}}\,\frac{g_1}{g_2}\,\frac{\lambda_{2j}}{\lambda_{1i}}, \tag{19}$$

where the statistical weights g_1 and g_2, and the wavelengths λ_{1i} and λ_{2j} are known.

This method directly yields the relative A values of the lines originating from two different energy levels without involving cumbersome absolute measurements. It was shown in Ref. 10 that the error occurring in such relative measurements could routinely be made less than 1%.

For this particular experiment, altogether nine such measurements were made, since there are nine different laser transitions between the $3s_2$ level and nine of the ten $2p$ levels (transition to $2p_9$ is forbidden). The $3s_2$-$2p_4$ transition at 632.8 nm was chosen for I_{1i} as a common reference and the intensity of the lines belonging to the $3p$-$3s$ transition array was compared with this reference line, producing a set of relative transition probabilities $A(2p_i - 1s_j)/A_{632.8}$ for all the lines except for the $2p_9$-$1s_5$ line at 640.2 nm. The value $A_{632.8} = (0.339 \pm 0.014) \times 10^7$ sec^{-1}, which was obtained from our previous measurements,[10] was used to place these relative values on an absolute scale.

III. EXPERIMENTS

The experimental arrangement is identical to that described in Ref. 10, and hence will not be described here in detail. The $\frac{1}{2}$-m Ebert scanning spectrometer is mounted with a 1180-lines/mm grating blazed at 750 nm, and its spectral dispersion is 1.6 nm/mm. Both entrance and exit slits were set at 25 μm. A filter (low-wavelength cutoff at 500 nm) was used to prevent the second-order spectra from entering the system. It was noticed that Rowland ghosts due to grating defects were present at the second and the fourth order with intensities as high as 0.25% of a parent line. In fact ghosts from several strong lines were comparable in size to some weak lines and on occasion complicated the identification of certain transitions. Fortunately none of the ghosts overlapped the desired lines.

Mixing in helium and argon will produce additional spectral lines that must be discriminated. The helium line at 667.8 nm ($3\,^1D$-$2\,^1P$), for instance, totally coincided with one of the neon lines ($2p_4$-$1s_2$). Also a similar case was seen with the neon line at 665.2 nm ($2p_3$-$1s_2$) and an unidentified line, possibly from argon. This problem was difficult to alleviate since removing argon from the gas mixture, in turn, created another problem of self-absorption. In this case, the relative intensity was measured by extrapolation to the zero current in a pure-neon discharge at reduced pressure.

First, the relative intensity of lines arising from the same upper level was measured in a Ne-Ar mixture at the total pressure of 0.4 Torr with the argon partial pressure of 0.1 Torr. Five runs were made at the discharge current, 15 mA, and each measurement agreed within 1%. Also, the discharge current was varied to see if there was a change in the intensity ratio due to the self-absorption effect, but no such change was observed. Effectiveness of argon for quenching the neon metastable states was discussed in Refs. 7, 10, and 11. Transitions were arranged into groups in which the lines share a common upper level. Intensity ratios of the lines from the same group reduce directly to the ratios of the transition probabilities because of simple cancellation of the population term. Despite the process being straightforward, a significant degree of discrepancy has been seen among the various data reported to date. This is mainly caused by the self-absorption effect and also possibly by inadequate detector calibration.

In order to place these relative values belonging to the different groups on a common relative scale, one transition was judiciously selected from each group and its intensity was compared with the reference line, the $3s_2$-$2p_4$ transition at 632.8 nm, under the specific plasma condition dictated by Eq. (16). This condition of transparency can be created in a He-Ne-Ar mixture at a wide range of discharge conditions. For instance, the gas mixture at 1.4 Torr in which the He-Ne ratio is 1 to 2 and the argon partial pressure is 0.1 Torr may become transparent at a discharge current of approximately 5 mA for a discharge tube with a 4-mm-bore diameter. Experimentally, this condition was verified by monitoring the intensity change of the 632.8-nm line, $\Delta I_{632.8}$, in the side-light emission from the discharge tube. The detection of the null ($\Delta I_{632.8} = 0$) was found to be highly sensitive. In our setup, 1% error in the null ($\Delta I_{632.8}/I_{632.8} = 0.01$, instead of its being exactly zero) amounted to less than 1% error in the population ratio N_1/N_2 (instead of its being exactly equal to g_1/g_2).

The wavelengths of the spectral lines involved in this experiment range from 540 to 808 nm. However, these two lines at the both ends of the spectral region are extremely weak, and all the stronger lines are concentrated within a much narrower range spanning some 160 nm between 585 and 744 nm. A photomultiplier tube with an S-20 response can comfortably cover all of these spectral lines without tasking the detector system too severely. The detector system (condenser lens, filter, grating monochromator, photomultiplier, picoammeter, and strip-chart recorder) was calibrated against a quartz-iodine standard lamp whose spectral irradiance curve is traceable to the primary standard.

Since the experiment involves only the relative intensity measurements of the type given in Eq. (19), the system calibration pertinent to this experiment is the relative spectral response $R(\lambda)$, which is normalized so that $R(632.8) = 1$. Such relative response is highly reproducible. The only element that affects the reliability of $R(\lambda)$ is the change in the relative output of the spectral irradiance lamp. The relative spectral radiancy depends only on absolute temperature T of the lamp, which depends in turn on the filament current i. Assuming a blackbodylike radiation for the lamp (equivalent blackbody temperature is rated 3000°K), it can be shown that $T \propto i^{1/2}$, and furthermore, it can also be shown that the relative output at wavelength λ, located some 100 nm away from the reference wavelength at 632.8 nm, will experience a change only by 0.6% when the current is offset from the rated value by 1%. The lamp current was checked against a laboratory standard and it was confirmed that its fluctuation was much less than 1% about the rated value. Hence, it is safe to conclude that the error included in the detector-system calibration is at worst 1 to 2%, and it is the greatest source of the systematic error in this experiment.

IV. RESULTS AND DISCUSSIONS

The relative A values $A(2p_i\text{-}1s_j)/A_{632.8}$ were normalized by using our previously measured value $A_{632.8} = (0.339 \pm 0.014)\times 10^7\ \text{sec}^{-1}$. The uncertainty is estimated to be 2% for the relative values and 6% for the absolute values, except for a few weak lines at 665.2 and 808.2 nm, where it is 10%. For the purpose of comparison, the results of recent experimental as well as theoretical work are shown along with our data in Table I.

The experiment of Bridges and Wiese[7] was conducted using the wall-stabilized arc of neon and argon. The transitions originating from the different $2p_i$ levels were linked up through a common temperature value based on local thermodynamic equilibrium. Their absolute scale was established by normalizing to the total transition probability sum obtained from the lifetime measurements of Bennett and Kindlmann[6] (our absolute scale is also dependent on these measurements). As one might notice, agreement between their data and ours is within the specified error limits throughout. Except for the $2p_3\text{-}1s_2$ line, the average deviation from our values is 3.3%. We note, however, that the values for the $2p_2$- and $2p_8$-level groups show rather large disagreement suggesting a possible influence from systematic errors in either one of the data sets.

The data set of Mehlhorn[3] is based on the intermediate coupling calculations. The wave functions were obtained by numerical fitting with both observed energies and Landé g values of the $2p_i$ levels. Its absolute scale was established by the radial transition integral value σ^2 obtained from the Coulomb approximation.[12] Agreement with our data is astonishingly good for medium to stronger lines, where the average deviation is 4.1%. One can notice, however, that agreement becomes very poor on weaker lines, implying that the wave functions were not accurate enough. Also it should be noted that the values are consistently smaller by about 2% on the average than our corresponding values, because σ^2 used by Mehlhorn is 6.52 (a.u.) whereas our average σ^2 is 6.66, differing by about 2%. This discrepancy, however, is within the error limit of the lifetime data of Bennett and Kindlmann on which our absolute scale was based.

The last data set is from the most recent intermediate coupling calculations conducted by Feneuille *et al.*[4] They have introduced a correction term of the form $\alpha L(L+1)$, which arises from long-range configuration interaction of the $2p^5 3p$ electron. Because of the correction term, significant improvement was realized in fitting the energy levels and Landé g values. Instead of the Coulomb approximation,[12] however, σ^2 was calculated by means of a parametrically fitted central-field potential. Accordingly a value, $\sigma^2 = 7.44$, significantly greater than that of the Coulomb approximation (6.60) has resulted. Hence, their original A values are about 10% greater than the rest of the data. Since we are interested in general agreement of the relative values, we took the liberty to force the data of Feneuille *et al.* to agree with our $2p_9\text{-}1s_5$ transition probability. Subsequently, the average deviation from our data is found to be 3.0%, except for the two weak lines at 540.1 and 665.2 nm, where the deviation is 25%. Improvement over Mehlhorn's calculations is evident especially on weaker lines. Furthermore, better consistency is seen with our data than any other data set in the table. As for the 10% disagreement over the absolute scale, it is definitely beyond the error margin of our data. It is, however, premature to answer at this stage whether the Coulomb approximation is superior to the method used by Feneuille *et al.* The Coulomb approximation seems to give much closer agreement with Bennett and Kindlmann's lifetimes,[6] which have been regarded thus far as being the most accurate experimental lifetime data. Further discussion on this point will follow later in this section.

We proceed, in the following, to carry out comparisons and analysis of our data in a manner similar to that undertaken by Bridges and Wiese.[7]

For the $2p^5 3p\text{-}2p^5 3s$ transition array of Ne I, the transition probability A_{ps} may be given by

$$A_{ps} = (64\pi^4/3h\lambda^3 g_p) S_{ps}\,, \tag{20}$$

where g_p is the statistical weight of the $3p$ levels, which is equal to $(2J_p+1)$. The line strength S_{ps}

is the square of the matrix element of the electric dipole operator $P = rO(\theta, \phi)$. In the central-field approximation, the transition integral may be separable into the angular part and the radial part; hence the line strength may be written as

$$S_{ps} = \langle 2p^5 3p\Psi | O(\theta, \phi) | 2p^5 3s\Psi' \rangle^2 \sigma^2, \tag{21}$$

where Ψ, Ψ' are the angular wave functions, $O(\theta, \phi)$ is the angular part of the operator P, and the radial transition integral σ^2 is given by

$$\sigma^2 = \frac{\langle nl|r|n'l'\rangle^2}{(4l_>^2 - 1)}, \tag{22}$$

where $l_>$ is the greater of the two azimuthal quantum numbers l and l' ($l_> = 1$ in this particular case).

The line strengths were calculated from Eq. (20) using the experimental transition probabilities of Table I, and are shown in Table II. Also shown are the so-called J-file sums: the line strengths were summed along each column ($\sum_p S_{ps}$), as well as along each row ($\sum_s S_{ps}$). According to Shortley,[1]

TABLE I. Absolute transition probabilities for the $2p_i$-$1s_j$ lines of Ne I. Some of the recent experimental and theoretical results are also shown for comparison.

Transitions	λ (nm)	This expt. (10^7sec^{-1})	(Experimental) Bridges and Wiese (Ref. 7)	(Theoretical) Mehlhorn (Ref. 3)	Feneuille *et al.* (Ref. 4)
$2p_1$-$1s_4$	540.056	0.090	0.090	0.046	0.067[a]
s_2	585.249	6.82	7.06	6.59	6.67
$2p_2$-$1s_5$	588.190	1.15	1.02	1.12	1.18
s_4	603.000	0.561	0.512	0.510	0.589
s_3	616.359	1.46	1.41	1.51	1.54
s_2	659.895	2.32	2.25	2.14	2.15
$2p_3$-$1s_4$	607.434	6.03	5.83	5.90	5.96
s_2	665.209	0.029	0.034	0.025	0.036
$2p_4$-$1s_5$	594.483	1.13	1.12	1.26	1.19
s_4	609.616	1.81	1.79	1.66	1.87
s_2	667.828	2.33	2.31	2.31	2.24
$2p_5$-$1s_5$	597.553	0.351	0.349	0.378	0.332
s_4	612.845	0.067	0.070	0.108	0.061
s_3	626.650	2.49	2.54	2.28	2.46
s_2	671.704	2.17	2.17	2.19	2.18
$2p_6$-$1s_5$	614.306	2.82	2.85	2.68	2.92
s_4	630.479	0.416	0.424	0.531	0.406
s_2	692.947	1.74	1.74	1.73	1.72
$2p_7$-$1s_5$	621.728	0.637	0.601	0.585	0.634
s_4	638.299	3.21	3.16	3.15	3.25
s_3	653.288	1.08	1.06	1.16	1.03
s_2	702.405	0.189	0.196	0.136	0.185
$2p_8$-$1s_5$	633.443	1.61	1.80	1.59	1.66
s_4	650.653	3.00	2.98	2.97	2.99
s_2	717.394	0.287	0.321	0.179	0.282
$2p_9$-$1s_5$	640.225	(5.14)[b]	5.06	5.06	5.14
$2p_{10}$-$1s_5$	703.241	2.53	2.53	2.53	2.55
s_4	724.517	0.935	1.00	0.930	0.953
s_3	743.890	0.231	0.242	0.222	0.234
s_2	808.246	0.012	0.012	0.008	0.011
Estimated error		6%[c]	10%[d]	...	...

[a]This data set was forced to agree for the $2p_9$-$1s_5$ transition of our data. The actual values were 11.6% larger.

[b]This value was not observed in our measurement, but it is an accurate estimation obtained through application of the J-file–sum rule. See the text for details.

[c]The estimated uncertainty for the two weak lines, at 665.2 and 808.2 nm, is 10%.

[d]The estimated uncertainty for the 540.0-, 665.2-, and 808.2-nm lines is 15%.

such J-file sums will be proportional to the statistical weights of the respective levels g_p or g_s. It can be shown that, for the $3p$-$3s$ array of Ne I,

$$\sum_s S_{ps} = g_p \sigma^2 \quad \text{and} \quad \sum_p S_{ps} = 3g_s \sigma^2. \tag{23}$$

In the $1s_5$ column on the table, the line strengths sum up to the partial sum of $8\sigma^2$ instead of the complete sum of $15\sigma^2$, since the $2p_9$-$1s_5$ transition was not covered in our experiment. Therefore, the over-all sum of our line strengths will be $29\sigma^2$, instead of $36\sigma^2$ as expected for the complete array. From this relationship one may calculate σ^2 using the experimental over-all line-strength sum. From the table we have $29\sigma^2 = 193.048$, and hence $\sigma^2 = 6.66$ a.u. Using this value of σ^2, one can extrapolate the missing line strength of the $2p_9$-$1s_5$ transition assuming that $S(2p_9\text{-}1s_5) = 7\sigma^2$ exactly. We have, thus, $S(2p_9\text{-}1s_5) = 46.598$ and, using Eq. (20), we obtain $A(2p_9\text{-}1s_5) = 5.14 \times 10^7$ sec^{-1}. Since the average deviation of the J-file sums from the corresponding $g_p\sigma^2$ and $3g_s\sigma^2$ is only 1.4% (with maximum deviation being 2.7% in the $1s_2$ column), the above assumption may be well justified. The resultant uncertainty of the estimated line strength will be 1–2%, unless this particular transition behaves anomalously different from the rest. However, this does not seem to be the case according to the other experimental data.

In the central-field approximation, σ^2 remains the same for a given transition array. Hence the angular part of the matrix element can be calculated by dividing each line strength by σ^2: $S_{ps}/\sigma^2 = \langle 2p^5 3p\Psi | O(\theta, \phi) | 2p^5 3s\Psi' \rangle^2$. The relative line strength S_{ps}/σ^2 obtained in this manner will now sum up to the statistical weights g_p or $3g_s$ of the respective rows and columns, the over-all sum being exactly equal to 36. From Eq. (23), it is straightforward to show that

$$\sum_s (S_{ps}/\sigma^2) = g_p,$$
$$\sum_p (S_{ps}/\sigma^2) = 3g_s, \tag{24}$$
$$\sum_s \sum_p (S_{ps}/\sigma^2) = \sum_p g_p = \sum_s 3g_s = 36.$$

It is more proper to compare these relative line strengths rather than the absolute A values as done in Table I, since all the values are now placed on the same relative scale through normalization of the over-all sum to 36. The data in Table I are converted to the relative line strengths S_{ps}/σ^2 and presented in Table III. Except for a few weak lines, excellent agreement is seen between all the data sets.

The J-file sum of the relative line strengths will be equal to the statistical weight g_p or $3g_s$ of the corresponding level, provided there is no configuration interaction. Three sets of experimental

TABLE II. Absolute line strengths obtained with the relationship $S_{ps} = g_p(3h\lambda^3/64\pi^4)A_{ps}$, where A_{ps} was taken from Table I. Also shown are the J-file sums $\sum_s S_{ps}$ and $\sum_p S_{ps}$, and the statistical weights of the corresponding levels.

Upper levels	$1s_2$	Line strengths $1s_3$	(a.u.) $1s_4$	$1s_5$	J-file sums $\sum_s S_{ps}$	g_p
$2p_1$	6.748		0.070		6.818	1
$2p_2$	9.872	5.076	1.821	3.451	20.220	3
$2p_3$	0.043		6.669		6.712	1
$2p_4$	17.152		10.125	5.880	33.157	5
$2p_5$	9.741	9.074	0.227	1.108	20.150	3
$2p_6$	14.299		2.573	16.130	33.002	5
$2p_7$	0.970	4.467	12.362	2.266	20.065	3
$2p_8$	2.614		20.369	10.124	33.107	5
$2p_9$				(46.598)[a]	(46.598)[a]	(7)
$2p_{10}$	0.094	1.411	5.267	13.045	19.817	3
					$\sum_p \sum_s S_{ps} =$	
$\sum_p S_{ps}$	61.533	20.028	59.483	52.004 (98.602)[b]	193.048 (239.646)[b]	
$3g_s$	9	3	9	8 (15)[c]		29 (36)[c]

[a]This value was not a measured value. It was calculated assuming that the J-file–sum rule held rigidly for this transition array.
[b]The values in parentheses include the calculated line strength of the $2p_9$-$1s_5$ transition.
[c]The values in parentheses include the statistical weight of the $2p_9$ level; $g(2p_9) = 7$.

data are compared on Table IV: our data, the data of Bridges and Wiese, and the third data set obtained by combining Bennett and Kindlmann's lifetime measurements and our relative A values. Each one involved a different method of interconnecting between different upper levels. As for the third data set, our relative A values were normalized individually to the lifetimes of the respective upper levels obtained by Bennett and Kindlmann.

All three sets seem to fulfill the J-file–sum rule very well as expected. Average deviations from the respective statistical weights are found to be 1.1% for our experiments, 1.9% for the data set of Bridges and Wiese, and 2.1% for the third data set. The values of our experiments, having a maximum individual deviation of only 2.7% (which is congruent with the error margin of our experiments), satisfy the J-file–sum rule most consistently, while some anomalously large deviations, up to 7.3%, can be seen in the other data sets (the $2p_1$ row of Bridges and Wiese and the $2p_3$ and $2p_{10}$ rows of Bennett and Kindlmann).

The J-file–sum rule may not be fulfilled owing either to the experimental error, or to configuration interaction. Judging from the fact that there seems to be no fixed trend between the three sets of data, however, it is reasonable to conclude that the experimental errors are the primary cause of the deviation from the J-file–sum rule. The error incurred during interconnecting the different $2p_i$ levels will directly show up as such deviations from the J-file–sum rule. A small but very subtle trend in our data set, that the partial J-file sums for the $2p_i$ levels incline toward somewhat smaller

TABLE III. Comparison of relative line strengths. The total line-strength sum $\sum_p \sum_s S_{ps}$ is normalized to 36, the over-all sum of the statistical weights of the $2p$ levels. The relative values, in this case, are equal to the square of the angular part of the matrix elements: $\langle 2p^5 3p\Psi | O(\theta,\phi) | 2p^5 3s\Psi' \rangle^2$.

Transitions	λ (nm)	This expt.	Bridges and Wiese (Ref. 7)	Mehlhorn (Ref. 3)	Feneuille *et al.* (Ref. 4)
$2p_1$-$1s_4$	540.056	0.0105	0.0105	0.0055	0.009
s_2	585.249	1.014	1.050	0.999	0.993
$2p_2$-$1s_5$	588.190	0.518	0.462	0.517	0.534
s_4	603.000	0.274	0.250	0.254	0.288
s_3	616.359	0.763	0.733	0.803	0.801
s_2	659.895	1.483	1.440	1.396	1.377
$2p_3$-$1s_4$	607.434	1.002	0.967	1.000	0.993
s_2	665.209	0.0064	0.0075	0.0056	0.009
$2p_4$-$1s_5$	594.483	0.883	0.877	1.001	0.933
s_4	609.616	1.521	1.504	1.423	1.569
s_2	667.828	2.577	2.542	2.603	2.496
$2p_5$-$1s_5$	597.553	0.167	0.165	0.183	0.156
s_4	612.845	0.0341	0.0357	0.0564	0.030
s_3	626.650	1.363	1.393	1.273	1.344
s_2	671.704	1.463	1.465	1.506	1.467
$2p_6$-$1s_5$	614.306	2.423	2.452	2.350	2.505
s_4	630.479	0.387	0.393	0.503	0.378
s_2	692.947	2.148	2.151	2.178	2.118
$2p_7$-$1s_5$	621.728	0.341	0.320	0.319	0.339
s_4	638.299	1.857	1.835	1.859	1.878
s_3	653.288	0.671	0.659	0.734	0.639
s_2	702.405	0.146	0.150	0.107	0.144
$2p_8$-$1s_5$	633.443	1.521	1.700	1.529	1.560
s_4	650.653	3.060	3.054	3.095	3.054
s_2	717.394	0.393	0.441	0.250	0.387
$2p_9$-$1s_5$	640.225	(7)	6.905	7.032	7.000
$2p_{10}$-$1s_5$	703.241	1.960	1.956	1.997	1.968
s_4	724.517	0.791	0.847	0.803	0.804
s_3	743.890	0.212	0.221	0.207	0.213
s_2	808.246	0.0142	0.0141	0.0096	0.012

values as the index i increases, is noticeable, suggesting a slight wavelength dependence. This might imply that a possible systematic error of about 1% over the wavelength range of this experiment is present in the calibration of our detector spectral response. Also noticeable in all data sets is a trend that the partial J-file sums of the $1s_2$ level is greater than the statistical weight of the level, while that of the $1s_5$ level falls short, implying a possible existence of self-absorption amounting to 1–2%, despite the due precautions taken. On the other hand, configuration interaction would result in the variation of σ^2 over the different $2p_i$ levels, and hence it may as well lead to such a degree of inconsistency. However, none of these implications are yet conclusive.

In order to investigate this point more explicitly, we have calculated σ^2 for each of the $2p_i$ and $1s_j$ levels, using the relationships $\sigma^2 = \sum_s S_{ps}/g_p$ and $\sigma^2 = \sum_p S_{ps}/3g_s$. This procedure implicitly assumes that the J-file–sum rule is rigidly obeyed, while the deviations as seen in Table IV are absorbed by variations in σ^2. The result is shown in Table V along with the weighted average $\sigma^2 = \sum_p \sum_s S_{ps}/36$ and the standard deviation from this average. Since the absolute scale of these three data sets is derived from the same source, the values in the table may be regarded as relative values, and hence the direct comparison of σ^2's between the different sets is possible. Furthermore, excellent agreement between weighted average values is not surprising for this reason. Except for a few anomalies, excellent agreement is seen between the three data sets. However, there seems hardly any correlation between them on the variation of σ^2's.

We have plotted these σ^2's against the indices of the corresponding $2p$ levels as shown in Fig. 1. It can be readily noticed that the values belonging to the $2p_{4-7}$ and $2p_9$ levels are in excellent agreement, while comparatively large deviations are seen on the other levels. Especially, the singular

TABLE IV. Comparison of measured J-file sums $\sum_s S_{ps}$ with the statistical weights. The total sum $\sum_p \sum_s S_{ps}$ is normalized to 36.

Upper levels	g_p	This expt.	Bridges and Wiese (Ref. 7)	Bennett and Kindlmann with this expt.
$2p_1$	1	1.024	1.061	1.024
$2p_2$	3	3.038	2.884	2.919
$2p_3$	1	1.008	0.975	0.941
$2p_4$	5	4.981	4.925	4.904
$2p_5$	3	3.027	3.060	2.973
$2p_6$	5	4.958	4.996	5.019
$2p_7$	3	3.014	2.965	2.944
$2p_8$	5	4.973	5.194	5.086
$2p_9$	7	(7)[b]	6.905	6.970
$2p_{10}$	3	2.977	3.037	3.220
Sums	36	29.000[b]	36.000	36.000
Lower levels	($3g_s$)			
$1s_2$	9	9.244	9.261	9.153
$1s_3$	3	3.009	3.006	2.956
$1s_4$	9	8.936	8.897	8.929
$1s_5$	15(8)[b]	7.812	14.837	14.962
Sums	36	29.000[b]	36.000	36.000
Average deviation (%)		1.1	1.9	2.1

[a] The relative transition probabilities of our experiment belonging to the same upper level were individually normalized to the lifetimes of the $2p$ states obtained by Bennett and Kindlmann (Ref. 6), and then the line strengths were calculated from the absolute A values obtained in this way. Notice an anomalously large disagreement on the $2p_{10}$ level.

[b] The $2p_9$-$1s_5$ transition was not covered in this measurement, and hence the normalization was made for the partial sum of 29. As for the $1s_5$ level, the J-file sum was compared with the partial sum of 8.

deviation on the $2p_{10}$ level of Bennett and Kindlmann's value is hard to account for. There seems to be a slight correlation between plots of Bridges and Wiese and Bennett and Kindlmann. However, considering the error margins of their relative values (3 to 5%), it is premature to conclude that such a trend indeed reflects the influence of configuration interaction. Our data, on the other hand, exhibit the least deviations from the weighted average throughout the ten $2p$ levels. Since the error on our relative A values is 2%, we may estimate the uncertainty of our individual σ^2 to be also about 2% on the relative basis. Therefore the effect of configuration interaction upon σ^2 would show up explicitly only if it causes a variation of σ^2 greater than 2%. Except for the mild deviation noticeable on the $2p_1$ level, no such trend is pronounced in our plot. Hence, we may regard this margin of 2% variation in σ^2 as the upper limit of the relative magnitude of configuration interaction. If this is indeed the case, then still higher experimental accuracy may be necessary to reveal the fine detail of such effects. Consequently, we proceed in the following discussion assigning just one value of σ^2 for this transition array, since the effect of configuration interaction seems to be within the error margin of our experiments. The most appropriate value may be the weighted average $\sigma^2 = 6.66 \pm 0.20$ a.u., where the uncertainty of about 3% is mainly due to the error in the lifetime measurements of Bennett and Kindlmann which provided the absolute scale.

According to the Coulomb approximation,[12] one obtains $\sigma^2 = 6.60$ for the center of gravity of the $2p^5 3p$ energy configuration. This is in exceedingly good agreement with the experimental value given above. On the other hand, Feneuille *et al.*[4] rejected the Coulomb approximation in favor of their own method of evaluation based on their central-field potential. The resultant σ^2 turned out to be 7.44, which is much larger than the values obtained from either the Coulomb approximation or the experiments. Their second-order corrections to account explicitly for the configuration interaction seems to have reduced this value by 5% or so, but the new value is still beyond the range of the 3% error limit of our σ^2. Under these circumstances it seems likely that this central-poten-

TABLE V. The radial transition integral σ^2 for both upper and lower levels.

	This expt.	Bridges and Wiese (Ref. 7)	Bennett and Kindlmann with this expt.	Coulomb approx. (a.u.) (Ref. 12)	Feneuille *et al.* (a.u.) (Ref. 4)
Upper level					
$2p_1$	6.82	7.05	6.86		
$2p_2$	6.74	6.39	6.52		
$2p_3$	6.71	6.48	6.30		
$2p_4$	6.63	6.55	6.57		
$2p_5$	6.72	6.78	6.64		
$2p_6$	6.60	6.64	6.72	6.60	7.44
$2p_7$	6.69	6.57	6.57		
$2p_8$	6.62	6.91	6.81		
$2p_9$	(6.66)[b]	6.56	6.67		
$2p_{10}$	6.61	6.73	7.19		
Lower level					
$1s_2$	6.84	6.84	6.81		
$1s_3$	6.68	6.66	6.60		
$1s_4$	6.61	6.57	6.65		
$1s_5$	6.50[b] (6.57)	6.58	6.68		
Average σ^2	6.66	6.65	6.70		
Std. dev. (%)	1.4 (1.2)[b]	2.7	3.0		

[a] To calculate σ^2, our relative A values were individually normalized to the lifetimes of the $2p$ states obtained by Bennett and Kindlmann (Ref. 6).

[b] The $2p_9$-$1s_5$ transition was not covered by our experiment. The value given in parentheses is obtained by application of the J-file–sum rule. The value for the $1s_5$ level is based on the partial line-strength sum and the value in the parentheses was obtained when the estimated value for the $2p_9$ level was included.

tial approximation is less suitable than the Coulomb approximation.

In Table VI our transition probability sums, $\sum_s A_{ps} = \tau_p^{-1}$, are shown along with other results from both experimental and theoretical works. Since all the experimental works share the common absolute-scale reference (Bennett and Kindlmann's lifetime scale), we have normalized the theoretical results to our value for the $2p^9$ level. The procedure is equivalent to aligning all the σ^2's of these data sets to our value, $\sigma^2 = 6.66$. The other two sets of experimental data possess values of σ^2 which are almost identical to ours. All the first five data sets show remarkably good agreement. Especially, our data and the two theoretical calculations agree within 1% except for the $2p_1$ level. The data set with the heading "Feneuille *et al.* II" is the original results of their second-order approximation.[4] Although the values were considerably reduced from the first-order result, one can notice significant discrepancy with the other data sets. However, it is interesting to note that, if these values were further reduced by 5% throughout, they practically coincide with the values of Bennett and Kindlmann. We are unable to explain whether this is accidental. In order to spot any systematic characteristics between the five data sets, we have also prepared them in the form of the diagram as shown in Fig. 2. The comparison may become more interesting if Fig. 2 is viewed along with Fig. 1. It can be immediately observed that all the data sets agree well on the levels $2p_{4-7}$ and $2p_9$, whereas agreement is not as good on the levels $2p_{1-3}$, $2p_8$, and $2p_{10}$. Because of the normalization to the common σ^2 value, Mehlhorn's data[3] became quite close to the data of Feneuille *et al.*[4] This is understandable because the transition probability sums would not be affected greatly by the weaker lines where Mehlhorn's calculation was found unsatisfactory. While our data are in excellent agreement with these two sets of theoretical data, the experimental data of Bridges and Wiese[7] and Bennett and Kindlmann[6] show behavior somewhat inconsistent with the theory. Also, they exhibit a similar over-all trend that was noticed in Fig. 1. Since the wavelengths of the transitions from a

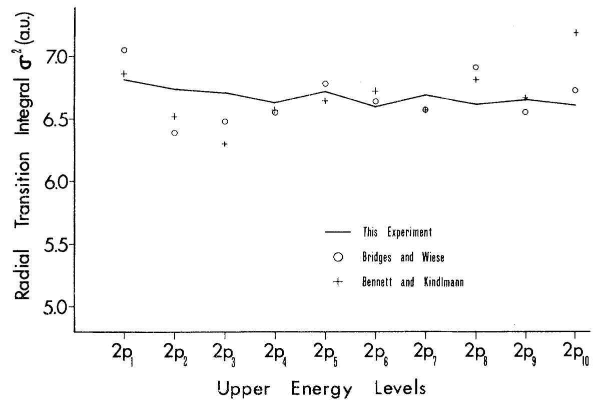

FIG. 1. Radial transition integrals for the individual $2p_i$ levels.

TABLE VI. Transition probability sums: $\sum_s A_{ps} = \tau^{-1} (10^7 \text{ sec}^{-1})$.

Upper level	This expt.	Experimental: Bridges and Wiese (Ref. 7)	Experimental: Bennett and Kindlmann (Ref. 6)	Theoretical: Mehlhorn [a] (Ref. 3)	Theoretical: Feneuille *et al.* I [b] (Ref. 4)	Theoretical: Feneuille *et al.* II [c] (Ref. 4)
$2p_1$	6.91	7.15	6.95	6.74	6.74	7.33
$2p_2$	5.49	5.19	5.32	5.44	5.46	5.61
$2p_3$	6.06	5.86	5.69	6.01	6.00	6.00
$2p_4$	5.28	5.22	5.23	5.31	5.29	5.50
$2p_5$	5.08	5.13	5.02	5.02	5.03	5.32
$2p_6$	4.98	5.01	5.07	5.01	5.04	5.32
$2p_7$	5.12	5.02	5.03	5.10	5.10	5.37
$2p_8$	4.90	5.10	5.04	4.96	4.93	5.25
$2p_9$	(5.14) [d]	5.06	5.15	5.14	5.14	5.40
$2p_{10}$	3.74	3.78	4.04	3.74	3.74	4.23
σ^2	6.66	6.65	···	6.66	6.66	7.04

[a] Numbers shown here are converted from the original data by means of normalizing to our radial transition integral $\sigma^2 = 6.66$, whereas the original σ^2 was 6.52.

[b] This data set is also normalized to our radial transition integral $\sigma^2 = 6.66$, whereas the original σ^2 of their first-order approximation was 7.44.

[c] Original results of their second-order approximation. The average value of σ^2 is 7.04, which is some 6% greater than the value from the Coulomb approximation.

[d] This value was estimated from the J-file–sum rule.

given upper level are relatively close to each other, σ^2 is roughly directly proportional to the transition probability sum, and hence the systematic trend observed on σ^2's should consequently show up in Fig. 2. The error in the individual line strengths has little to do with the discrepancy seen here, but rather the error that arose when the different $2p$ levels were interconnected would be mostly responsible for it. We shall not attempt here to determine which set of the experiment included the greater error, but mention that the estimated errors in the relative lifetime values is 2% in our experiment, whereas it is about 3% in the other experiments. It is also possible that the deviations in the $2p_{1-3}$ and $2p_{10}$ levels may well be attributable to configuration interaction since these levels are located relatively far from the position of the center of gravity of the $2p^5 3p$ energy configuration.

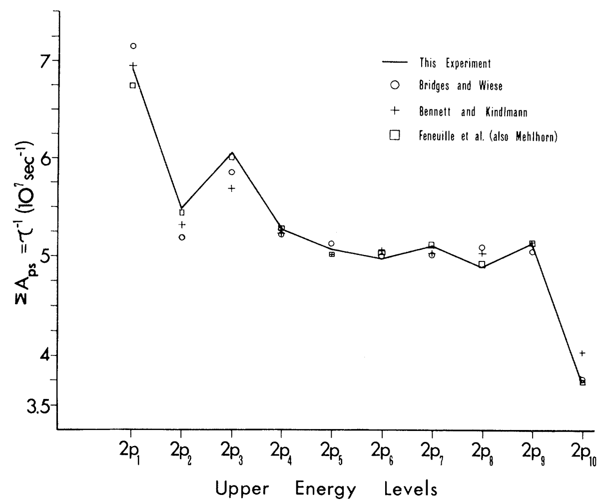

FIG. 2. Transition probability sums (inverse lifetimes) plotted against index of corresponding $2p_i$ levels. The data of Mehlhorn are deliberately omitted, since it practically coincides with the plots of Feneuille *et al.* This was necessary to avoid confusion.

V. CONCLUSIONS

An experimental method of measuring transition probabilities of spectral lines belonging to two different upper levels has been described in detail. The method is based on the availability of a laser transition between the given energy levels under investigation. A rigorous theoretical analysis was presented in terms of rate equations, and their use was demonstrated on the nine sets of energy levels involving the $3s_2$ and the $2p_{1-8,10}$ levels of Ne I. As a result, the relative transition probabilities and the relative lifetimes of the spectral lines associated with the $2p^5 3p$-$2p^5 3s$ transition array were precisely determined against one reference value, $A_{632.8}$. These relative values are significant by themselves in the sense that the methods of linking up the various $2p_i$ levels are uniquely different from the conventional ones. However, by combining these values with the accurate lifetimes of Bennett and Kindlmann, a series of important spectroscopic data has resulted with accuracy never attained before.

The data of significant importance are the absolute transition probabilities of the 30 lines associated with the $3p$-$3s$ array, the radial transition integral, and the radiative lifetimes of the ten energy levels belonging to the $3p$ configuration.

These results were subsequently subjected to extensive comparisons with recent experimental as well as theoretical results, and the results of this experiment were found to comply with several spectroscopic tests most consistently.

It is particularly noteworthy that all of these recent data sets, both experimental and theoretical, are in excellent agreement, and finally many problems associated with these neon spectra seem to have been settled. The angular-momentum coupling scheme in neon is indeed complex. None of the simple pure coupling schemes such as *jj*, *jl*, etc., could adequately describe the process. The intermediate coupling scheme of Shortley and the recent approaches taken by Murphy, Mehlhorn, and Feneuille *et al.* seem to be able to cope with this problem successfully. The recent improvement on the intermediate coupling theory achieved by Feneuille *et al.*, in particular, has reached the point where agreement between the experiments and the theory is quite acceptable as far as the relative line strengths (or the angular part of the transition matrix elements) are concerned.

As for the radial part of the transition integral, the Coulomb approximation seems to produce the right result. On the other hand, however, the radial factors of Feneuille *et al.* obtained from the semiempirical central-field potential, although they are slightly larger, are also in reasonable agreement with the experiments. It is vitally important that a new set of lifetimes, which surpasses the accuracy of Bennett and Kindlmann's results, should be measured. The results of this experiment indicate that configuration interaction on the $2p^5 3p$ states is very small. However, the detailed account of configuration interaction is yet to be revealed pending the advent of a more accurate set of lifetime data.

*Work partially supported by grants from AFOSR and Research Corporation.

†Work based in part on a dissertation submitted by S. Inatsugu in partial fulfillment of the requirements for the Ph.D. degree at the University of Hawaii.

[1]E. U. Condon and G. H. Shortley, *The Theory of Atomic Spectra* (Cambridge U.P., Cambridge, England, 1967), Ch. XI.

[2]P. W. Murphy, J. Opt. Soc. Am. 58, 1200 (1968).

[3]R. Mehlhorn, J. Opt. Soc. Am. 59, 1453 (1969).

[4]S. Feneuille, M. Klapisch, E. Koenig, and S. Lieberman, Physica 48, 571 (1970).

[5]We avoid individual listings of the papers. For details refer to Bibliography on Atomic Transition Probabilities [Natl. Bur. Stand. (U.S.), Washington, D. C.]. Original issue by B. M. Glennon and W. L. Wiese, 1966. Supplements 1 and 2 by J. R. Fuhr and W. L. Wiese, 1971 and 1973.

[6]W. R. Bennett, Jr. and P. J. Kindlmann, Phys. Rev. 149, 38 (1966).

[7]J. M. Bridges and W. L. Wiese, Phys. Rev. A 2, 285 (1970).

[8]T. Hänsch and P. Toschek, Phys. Lett. 20, 273 (1966).

[9]T. V. Bychkova, V. G. Kirpilenko, S. G. Rautian, and A. S. Khaikin, Opt. Spectrosc. 22, 371 (1967).

[10]S. Inatsugu and J. R. Holmes, Phys. Rev. A 8, 1678 (1973).

[11]P. E. Toschek, W. Hübner, and H. Schneider, LASER Report No. 1-72, Institute für Angwandte Physik, Universität Heiderberg (unpublished).

[12]D. R. Bates and A. Damgaard, Philos. Trans. R. Soc. Lond. A 242, 101 (1949).